

Journal of Electronic Materials

Catalytic graphitization for preparation of porous carbon material derived from bamboo precursor and performance as electrode of electrical double layer capacitor --Manuscript Draft--

Manuscript Number:	JEMS-D-15-00188
Full Title:	Catalytic graphitization for preparation of porous carbon material derived from bamboo precursor and performance as electrode of electrical double layer capacitor
Article Type:	Original Research
Keywords:	catalytic graphitization; activation; bamboo; electrochemical capacitor; carbon.
Corresponding Author:	Tohiki Tsubota, Ph.D. Kyushu Institute of Technology Kitakyushu, JAPAN
Corresponding Author Secondary Information:	
Corresponding Author's Institution:	Kyushu Institute of Technology
Corresponding Author's Secondary Institution:	
First Author:	Tohiki Tsubota, Ph.D.
First Author Secondary Information:	
Order of Authors:	Tohiki Tsubota, Ph.D. Yuta Maguchi, Bachelor Sunao Kamimura, Ph.D. Teruhisa Ohno, Ph.D. Takehiro Yasuoka, Ph.D. Haruo Nishida, Ph.D.
Order of Authors Secondary Information:	
Funding Information:	
Abstract:	<p>The combination of the addition of Fe, which acts as catalyst for graphitization, and CO₂ activation, which is a kind of gaseous activation, was performed in order to prepare porous carbon material from bamboo powder which is the waste of superheated steam treatment. Regardless of the heat treatment temperature, many macropores were successfully formed by the removal of the Fe compounds after the heating process. The turbostratic carbon structure generated in the Fe-added sample heated at 850 degrees C. It was confirmed that the added Fe acted as the template for pore formation. Moreover, it was confirmed that the added Fe acted as the catalyst for graphitization. The electrochemical performances for the electrode of electrical double layer capacitor, such as cyclic voltammetry, electrochemical impedance spectroscopy, and charge-discharge test, could be explained by the effects of the graphitization and activation. The addition of Fe could affect the electrical property of the carbon material derived from bamboo.</p>
Suggested Reviewers:	Satoshi Kumagai, Ph.D. Saga University f9229@cc.saga-u.ac.jp He have studying the application of biomass such as bamboo. Nobuyuki Hayashi, Ph.D. Professor, Saga University yurika@cc.saga-u.ac.jp He has studying the treatment of bamboo with high pressure hot water.

Seiichi Inoue
AIST
s.inoue@aist.go.jp
He is studying the hydrothermal treatment of biomass such as bamboo.

Yumiko Kodama
Tohoku University
kodama@imr.tohoku.ac.jp
She has reported "Electron microscope study of the formation of graphitic nanostructures in nickel-loaded wood char" (CARBON 50 (2012) 3486-3496)

1
2
3 **Catalytic graphitization for preparation of porous carbon material**
4
5 **derived from bamboo precursor and performance as electrode of**
6
7 **electrical double layer capacitor**
8
9

10
11
12 Toshiki Tsubota^{1*}, Yuta Maguchi¹, Sunao Kamimura¹, Teruhisa Ohno¹, Takehiro

13
14 Yasuoka², Haruo Nishida²
15
16

17
18
19 1: Department of Applied Chemistry, Faculty of Engineering, Kyushu Institute of
20
21 Technology
22

23
24 1-1 Sensuicho, Tobata-ku, Kitakyushu, Fukuoka 804-8550, Japan
25
26

27
28
29 2: Department of Biological Functions and Engineering, Graduate School of Life
30
31 Science and System Engineering, Kyushu Institute of Technology
32

33
34 2-4 Hibikino, Wakamatsu-ku, Kitakyushu, Fukuoka 808-0916, Japan
35
36

37
38 *: corresponding author
39

40
41 Toshiki Tsubota
42

43
44 e-mail: tsubota@che.kyutech.ac.jp
45

46
47 postal address: Department of Applied Chemistry, Faculty of Engineering, Kyushu
48
49 Institute of Technology, 1-1 Sensuicho, Tobata-ku, Kitakyushu, Fukuoka 804-8550,
50
51 Japan
52

53
54 Tel.: +81-93-884-3324, FAX: +81-93-884-3300
55
56
57
58
59
60

1
2
3 **Abstract**
4

5 The combination of the addition of Fe, which acts as catalyst for graphitization, and CO₂ activation,
6 which is a kind of gaseous activation, was performed in order to prepare porous carbon material from
7 bamboo powder which is the waste of superheated steam treatment. Regardless of the heat treatment
8 temperature, many macropores were successfully formed by the removal of the Fe compounds after the
9 heating process. The turbostratic carbon structure generated in the Fe-added sample heated at 850
10 degrees C. It was confirmed that the added Fe acted as the template for pore formation Moreover, It was
11 confirmed that the added Fe acted as the catalyst for graphitization. The electrochemical performances
12 for the electrode of electrical double layer capacitor, such as cyclic voltammetry, electrochemical
13 impedance spectroscopy, and charge-discharge test, could be explained by the effects of the graphitization
14 and activation. The addition of Fe could affect the electrical property of the carbon material derived
15 from bamboo.
16
17
18
19
20
21
22
23
24
25
26
27
28
29
30

31
32
33
34
35 **Keywords**
36

37 catalytic graphitization; activation; bamboo; electrochemical capacitor; carbon.
38
39
40
41
42
43
44
45
46
47
48
49
50
51
52
53
54
55
56
57
58
59
60
61
62
63
64
65

1
2
3
4
5 **1. Introduction**
6

7 The treatment with superheated steam is used as one of the pretreatments in the field of bioethanol
8 production [1]. Moreover, because hemicelluloses, which is one of the components in plants and binds
9 the cellulose fibrils, were degraded during the superheated steam treatment [2], bamboo fibers derived
10 from the plant tissue could be produced from bamboo by the superheated steam treatment. Some
11 researchers have prepared bamboo fibers, which were synthesized not by superheated steam, as a
12 reinforced polymer [3, 4]. Therefore, bamboo fibers produced by superheated steam could be used as
13 the filler for resin and polymers. However, the residue (bamboo powder), which has a small size (less
14 than 63 micrometers) and low-aspect ratio, should not be used.
15
16

17 The electrical double layer capacitor (EDLC) has attracted attention as an electrical energy storage
18 device. There are some advantages of the EDLC over a battery such as a high cycle characteristic, rapid
19 charge-discharge etc. However, in general, the capacitance of the EDLC is much lower than that of a
20 battery. Therefore, the improvement of the capacitance of the EDLC has been required for application
21 in various fields. Because the electrode, which is a carbon material, such as activated carbon in general,
22 should be one of the essential factors for the EDLC performance, the development of a high performance
23 electrode has been underway. So far, many materials have been used as the precursor for the carbon
24 electrode, such as the material derived from a fossil fuel, synthetic resin, and biomass. The biomass
25 should be preferable from the viewpoint of the prevention of global warming.
26
27

28 Carbon materials can be classified into two categories, that is, graphitizing carbon and non-graphitizing
29 carbon. Although non-graphitizing carbon cannot be graphitizable even at a high temperature (3000
30 degrees C), it can be catalytically graphitized by the addition of Fe at a relatively low temperature
31 (usually <1800 degrees C). Moreover, some experimental results indicated that the chemical structure of
32 the carbon material can be affected by the addition of Fe at a lower temperature [5]. It should be
33
34
35
36
37
38
39
40
41
42
43
44
45
46
47
48
49
50
51
52
53
54
55
56
57
58
59
60
61
62
63
64
65

1
2
3 presumed that turbostratic carbon and graphitized carbon have a higher electrical conductivity than
4
5 non-graphitizing carbon. Therefore, the internal resistance of an EDLC electrode may be suppressed by
6
7 these carbon structures. Moreover, if the Fe catalysts were removed after the carbonization process,
8
9 many pores may be introduced on the carbon material. Thus Suzuki et al. synthesized mesoporous
10
11 carbon using a Ni catalyst [6]. Therefore, the mesopore formation by an Fe catalyst can be expected.
12
13

14
15 It is known that non-graphitizing carbon can be easily activated whereas graphitizing carbon is resistant
16
17 to activation. That is, non-graphitizing carbon should be more suitable than graphitizing carbon for a
18
19 high specific surface area, which could enhance the capacitance value of the EDLC electrode although the
20
21 electrical conductivity of the non-graphitized carbon could be lower than that of the graphitized carbon.
22
23

24
25 In general, CO₂ activation forms micropore, resulting in a large specific surface area. Therefore, we
26
27 propose a method combining the addition of Fe (for partial graphitization and mesopore formation) and
28
29 CO₂ activation (for micropore formation in non-graphitized region) in order to improve the capacitance
30
31 value of the EDLC electrode. In this study, the combination of the addition of Fe and CO₂ activation
32
33 was attempted for the synthesis of a carbon material which has a high electrical conductivity and high
34
35 specific surface area for the EDLC electrode.
36
37
38
39
40

41 **2. Experimental**

42 **2.1 Bamboo powder produced by superheated steam process**

43
44
45 Bamboo was treated using a batch-type superheated steam apparatus (Dai-ichi High Frequency Co.,
46
47 Ltd.) at 210 degrees C for 3 h. After the superheated steam treatment, the bamboo was mechanically
48
49 crushed, then the crushed bamboo was sieved. The material screened out (less than 63 micrometers) is
50
51 called bamboo powder. As the starting material for the carbon material, the bamboo powder was used in
52
53 this study. An optical microscopy image is shown in Fig. s1. The contents of the bamboo powder
54
55 included *ca.* 45 wt.% cellulose, *ca.* 15 wt.% hemicellulose, and *ca.* 40 wt. % lignin.
56
57
58
59
60
61
62
63
64
65

2.2 Preparation of carbon material

The bamboo powder was added to distilled water with $\text{Fe}(\text{NO}_3)_3 \cdot 9\text{H}_2\text{O}$. The weight of the added Fe (not $\text{Fe}(\text{NO}_3)_3 \cdot 9\text{H}_2\text{O}$ but Fe) was 10 % of the bamboo powder weight. The suspension was dried in a dryer at 75 degrees C for more than 1 day. The dried powder was placed in an electrical furnace, then heated at 500 degrees C or 800 degrees C for 1 h under flowing N_2 (0.5 L min^{-1}). The sample after the heat treatment was stirred in an 11.4 M HCl aqueous solution at 65 degrees C for 3 hours. The sample treated with the HCl solution was collected by filtration and washed with distilled water. The washed sample was dried in the dryer at 75 degrees C for more than 1 day. The dried sample was placed in the electrical furnace again, and then the temperature increased to 850 degrees C under flowing N_2 (0.5 L min^{-1}). When the temperature attained 850 degrees C, the flowing gas was changed from N_2 to CO_2 (0.5 L min^{-1}). The temperature was then kept at 850 degrees C for 1 hour under the flowing CO_2 (0.5 L min^{-1}). The temperature then decreased to room temperature with the flowing N_2 (0.5 L min^{-1}). The sample was stirred in an 11.4 M HCl aqueous solution at 65 degrees C for 3 hours again, and the sample was collected by filtration and washed with distilled water. The washed sample was dried in the dryer at 75 degrees C for more than 1 day. In this study, the information about the treatment temperature was described on the label of the samples. For the sample with added Fe, "Fe" was written on the label. For example, when the bamboo powder mixed with $\text{Fe}(\text{NO}_3)_3 \cdot 9\text{H}_2\text{O}$ was heated at 500 degrees C and the sample was heated at 850 degrees C, the sample label was (500Fe-850).

2.3 Characterization

The microstructure of the samples was investigated using an FE-SEM (JEOL, JSM-6320F) and TEM (HITACHI, H-9000NAR). The N_2 adsorption isotherms (Quantachrome Instruments, NOVA4200e) were measured for estimation of the pore size distribution and BET specific surface area.

2.4 Electrochemical measurements

The synthesized carbon material was mixed with PTFE in order to form a sample sheet. The weight ratio of PTFE to the carbon material was 1/9. A few drops of N-methylpyrrolidone were used for the homogeneous dispersion of the PTFE. The sheet sample, the thickness of which was *ca.* 0.5 mm, was cut in the size of 20 mm * 8 mm for the electrochemical measurements, such as the cyclic voltammetry and charge-discharge test. These electrochemical measurements were performed in a three-electrode cell using a potentiostat/galvanostat (Toyo Corporation, VersaSTAT3). A 1 M H₂SO₄ aqueous solution, which was bubbled with N₂ gas before the electrochemical measurements, was used as the electrolyte. A Pt plate was used as the counter electrode, the sheet sample, which was pressed on another Pt plate in the cell was used as the working electrode, and a Ag/AgCl electrode was used as the reference electrode. The capacitance values were calculated from the charge process data of the charge process.

3. Results and discussion

The XRD patterns for the samples are shown in Fig. 1. There were broad peaks, which should be assigned to the non-graphitizing carbon, in the graph of sample (850-850). On the other hand, an obvious peak appeared at 26 degrees in the pattern for the sample (850Fe-850). The peak at 26 degrees should mean that a catalytic reaction occurred during the heating process. The other small peaks at 35-50 degrees could be assigned to the remaining Fe compounds such as Fe₂O₃ or turbostratic carbon. The peak position at 26 degrees and the shape corresponded to the T-effect, which means that turbostratic carbon exists in the sample. In the case of the Ni catalyst, the effect of the catalytic graphitization depended on the size of the catalyst [7]. When the Ni size was *ca.* 20 nm, the T-effect appeared in the carbon derived from the phenolic resin. On the other hand, when the Ni size was *ca.* 80 nm, the G-effect, which means that graphitic carbon exists in the sample, appeared in the carbon derived from the phenolic

1
2
3 resin. It is known that small-size Fe also acts as a catalyst for the T-effect via a dissolution-precipitation
4
5 mechanism. From this XRD measurement result, the size of the Fe catalyst in this study, therefore,
6
7 could be presumed to be low or middle double-digit nanometers.
8
9

10 There was a peak at 26 degrees in the XRD pattern for sample (850Fe-850). Therefore, both the
11
12 addition of Fe and the high temperature at 850 degrees C should be necessary for the graphitization, that
13
14 is, the Fe catalyst was inert at 500 degrees C. Charon et al. reported the effect of the addition of Fe and
15
16 the treatment temperature on the microstructure the carbon material [5]. When saccharose-based char
17
18 (obtained at 400 degrees C), which is a non-graphitizing carbon, was heated at 650 degrees C with Fe, the
19
20 treated carbon material had no turbostratic carbon. On the other hand, when the char mixed with Fe was
21
22 heated at 900 degrees C, the treated carbon material contained turbostratic carbon. Therefore, the
23
24 experimental results of this study were consistent with the reported results.
25
26
27
28
29
30

31 The SEM and TEM images of the samples are shown in Fig. 2. The sample prepared without the
32
33 addition of Fe had a smooth surface. On the other hand, there were many pores in the samples with
34
35 added Fe. These pores should be formed by the removal of Fe or Fe₂O₃ during the treatment with the
36
37 HCl aqueous solution. The TEM image for the sample indicated that Fe particles with diameters of low
38
39 double-digit nanometers existed in the sample. The size of the particle corresponded to that for the
40
41 T-effect, that is, *ca.* 20 nm.
42
43
44
45
46
47

48 The N₂ adsorption isotherms of the samples are shown in Fig. 3. The graphs for samples (850-850)
49
50 was type "I" defined by IUPAC. On the other hand, the graph for sample (850Fe-850) was type "II".
51
52 As for the sample (500Fe-850), the shape was the intermediate type between type "I" and type "II". The
53
54 drastically increment of the adsorbed amount at low relative pressure region, such as the "I" type, should
55
56 mean the existence of micropores (less than 2 nm). It is known that gaseous activation, such as CO₂,
57
58
59
60
61
62
63
64
65

1
2
3 produced micropores in the first step. Therefore, the CO₂ activation process should be effective for
4
5 samples (850-850) and (500Fe-850). The type "II" could mean the existence of macropores (more than
6
7 50 nm). This result should correspond to the SEM image of sample (850Fe-850). The pore size
8
9 distributions of the samples were calculated by DFT method, and those were shown in Fig. s2. Because
10
11 adsorption isotherms cannot measure large size pore, the existence of macropores could not be confirmed
12
13 from the data. However, the increment of the amount of mesopore with Fe addition should be confirmed
14
15 from Fig. s2.
16
17

18
19 The yields (weight of product)/(weight of bamboo powder) and the specific surface areas are listed in
20
21 Table 1. The yield of sample (850Fe-850) was less than those of the other samples after the first heat
22
23 treatment. The small yield of the sample of (500Fe-850) at the second heat treatment could be explained
24
25 by the activation reaction because the sample had the largest specific surface area. The specific surface
26
27 area of (850-850) was 966 m² g⁻¹, and this value is similar to the value reported for activated carbon
28
29 derived from bamboo [8, 9]. It should be noted that the specific surface area for sample (850Fe-850)
30
31 was lower than that for sample (850-850). It is known that the graphitized carbon is poorly activated.
32
33 The turbostratic carbon structure of sample (850Fe-850) should be the reason for the lower specific
34
35 surface area. The specific surface area for sample (500Fe)-(850) was much higher than that for sample
36
37 (850-850). Because sample (500Fe)-(850) was non-graphitized carbon, it was well activated during the
38
39 CO₂ activation process. Therefore, the calcination at 500 degrees C with the addition of Fe and then
40
41 CO₂ activation at 850 degrees C after removal of the Fe should be an effective process for the
42
43 enhancement of the specific surface area.
44
45
46
47
48
49
50
51
52

53 The CV graphs of the samples are shown in Fig. 4. All the graphs should indicate that these
54
55 electrodes charged through the medium of the electrical double layer because the shapes of the graphs
56
57 were nearly square. The graph of sample (850Fe-850) had the smallest area, and showed small humps
58
59
60
61
62
63
64
65

1
2
3 although the shape was most nearly square. The small humps may be derived from few Fe compounds
4
5 remaining in the sample. The (500Fe-850) sample had the largest area in the graphs. However, the
6
7 shape was the most distorted for sample (500Fe-850).
8
9

10
11
12 The current density dependence of the capacitance values are shown in Fig. 5. The sample of
13
14 (500Fe)-(850) had the highest value in the region of a low current density although the capacitance value
15
16 significantly decreased with the increasing current density. The sample of (850Fe-850) had a good rate
17
18 performance although the capacitance values were low. The relation between the specific surface areas
19
20 and the capacitance values at 10 mA g⁻¹ is shown in Fig. s3. The capacitance value per weight (F g⁻¹)
21
22 was proportional to the specific surface area, and the slope, that is, the capacitance value per area (F m⁻²),
23
24 was *ca.* 0.1 F m⁻². Centeno et al. reported the separation of the capacitance derived from electric double
25
26 layer and that derived from the CO-generating functional group [10]. The capacitance value per area (F
27
28 m⁻²) was almost constant in this study, the magnitude relation of the capacitance value per area in the
29
30 region of a low current density could be explained by the magnitude relation of the specific surface area.
31
32 Therefore, the value in this study could mean that most of the capacitance was derived from the electric
33
34 double layer.
35
36
37
38
39
40
41
42

43
44 Nyquist plots of the samples are shown in Fig. 6. The left intersection of the x axis and semicircle
45
46 represents the solution resistance (R_s), and the diameter of the semicircle represents the charge transfer
47
48 resistance (R_{ct}) [11]. The R_{ct} value is generally due to contact resistance between the electrode material
49
50 and current collector and interparticle resistance of the sample. Therefore, the internal resistance is
51
52 represented by ($R_s + R_{ct}$). One of the reasons for the low internal resistance of the (850Fe-850) sample
53
54 should be the existence of the turbostratic carbon. The rate performance (capacitance at 1000 mA
55
56 g⁻¹)/(capacitance at 10 mA g⁻¹) is listed in Table s1. The magnitude relation of the ($R_s + R_{ct}$) values
57
58
59
60
61
62
63
64
65

1
2
3 corresponded to the magnitude relation of the rate performance. This result should be reasonable
4
5 because the capacitance value in the region of the high current density should be strongly affected by the
6
7 internal resistance.
8
9

10
11
12 In this study, the capacitance value could not be improved by the method of combining the partial
13
14 catalytic graphitization and CO₂ activation. However, the effect of the catalytic graphitization and that
15
16 of the CO₂ activation were confirmed. Therefore, if the optimization of these effects was performed, a
17
18 high performance material should be synthesized.
19
20
21
22
23

24 The experimental results are summarized as follows,

- 25
26 1. The addition of Fe is effective for the formation of pores in the sample although the pores are
27
28 macropores regardless of the carbonization temperature.
29
30
- 31
32 2. The turbostratic carbon structure can be produced by the combination of the addition of Fe and the heat
33
34 treatment at 850 degrees C.
35
36
- 37
38 3. The combination of the carbonization at 500 degrees C with Fe-doping and the CO₂ activation was
39
40 effective for enhancing of the specific surface area.
41
42
- 43
44 4. The introduction of the turbostratic carbon structure is effective for improving the rate performance.
45
46
47

48 **Conclusions**

49
50 The addition of Fe to bamboo powder produced by superheated steam was attempted in order to control
51
52 the carbon structure. Many pores were introduced in the sample when the addition of Fe was performed
53
54 as a pretreatment. Moreover, the doped-Fe acted as a catalyst for the formation of the turbostratic
55
56 carbon structure when the carbonization treatment was at 850 degrees C. The combination of the
57
58
59
60

1
2
3 carbonization at 500 degrees C with Fe-doping and the CO₂ activation successfully enhanced the specific
4
5 surface area. The introduced turbostratic carbon structure improved the rate performance of the
6
7 capacitance value.
8
9

10 11 12 **Acknowledgment**

13
14 This work was supported by JSPS KAKENHI Grant Numbers 26410253 and The Yamagin Regional
15
16 Enterprise Support Foundation.
17
18
19
20
21
22
23
24
25
26
27
28
29
30
31
32
33
34
35
36
37
38
39
40
41
42
43
44
45
46
47
48
49
50
51
52
53
54
55
56
57
58
59
60

1
2
3 **References**
4

- 5 [1] O.J. Sa´nchez, C.A. Cardona, *Bioresource Technology* 99, 5270 (2008)
6
7 [2] N.I.A.A. Nordin, H. Ariffin, Y. Andou, M.A. Hassan, Y. Shirai, H. Nishida, W.M.Z.W. Yunus, S.
8
9 Karuppuchamy, N.A. Ibrahim, *Molecules* 18, 9132 (2013)
10
11 [3] S.K. Chattopadhyay, R.K. Khandal, R. Uppaluri, A.K. Ghoshal, *Journal of Applied Polymer Science*
12
13 119, 1619 (2011)
14
15 [4] C. Wang, S. Ying, *Fibers and Polymers* 15, 117 (2014)
16
17 [5] E. Charon, J.N. Rouzaud, J. Ale´on, *Carbon* 66, 178 (2014)
18
19 [6] T. Suzuki, K. Suzuki, Y. Takahashi, M. Okimoto, T. Yamada, N. Okazaki, Y. Shimizu, M. Fujiwara,
20
21 *Journal of Wood Science*, 53, 54 (2007)
22
23 [7] A. Oya, H. Marsh, *Journal of Materials Science*, 17, 309 (1982)
24
25 [8] J.C. Moreno-Pirajan, L. Giraldo, *Central European Journal of Chemistry*, 11, 160 (2013)
26
27 [9] R. Wang, Y. Amano, M. Machida, *Journal of Analytical and Applied Pyrolysis*, 104, 667 (2013)
28
29 [10] T.A. Centeno, F. Stoeckli, *Electrochimica Acta* 52, 560 (2006)
30
31 [11] R.S. Hastak, P. Sivaraman, D.D. Potphode, K. Shashidhara, A.B. Samui, *Electrochimica Acta* 59, 296
32
33 (2012)
34
35
36
37
38
39
40
41
42
43
44
45
46
47
48
49
50
51
52
53
54
55
56
57
58
59
60
61
62
63
64
65

1
2
3
4
5
6
7
8
9
10
11
12
13
14
15
16
17
18
19
20
21
22
23
24
25
26
27
28
29
30
31
32
33
34
35
36
37
38
39
40
41
42
43
44
45
46
47
48
49
50
51
52
53
54
55
56
57
58
59
60
61
62
63
64
65

Table 1 Specific surface areas and yields.

sample	$S_{\text{BET}} / \text{m}^2 \text{g}^{-1}$	Yield of first heat treatment / %	Yield of second heat treatment / %
850-850	966	40.0	21.3
850Fe-850	778	24.0	16.3
500Fe-850	1724	39.2	13.4

Table s1 Rate performances of the samples.

	10 mA g ⁻¹		1000 mA g ⁻¹		C_{1000}/C_{10}
	F g ⁻¹	F m ⁻²	F g ⁻¹	F m ⁻²	
850-850	120.8	0.125	71.5	0.074	0.591
850Fe-850	79.9	0.103	66.9	0.086	0.837
500Fe-850	156.7	0.091	53.3	0.031	0.340

1
2
3 **Figure captions**
4

5 Fig. 1 XRD patterns of the samples.
6

7 (a), sample of (850-850); (b), sample of (850Fe-850); (c), sample of (500Fe-850).
8
9

10 Fig. 2 SEM and TEM images of the samples.
11

12 (a), sample of (850-850); (b), sample of (850Fe-850); (c), sample of (500Fe-850);
13 (d), TEM image of sample of (850Fe-850).
14
15

16 Fig. 3 N₂ adsorption isotherms of the samples.
17

18 (a), sample of (850-850); (b), sample of (850Fe-850); (c), sample of (500Fe-850).
19
20

21 Fig. 4 CV graphs of the samples.
22

23 (a), sample of (850-850); (b), sample of (850Fe-850); (c), sample of (500Fe-850).
24
25

26 Fig. 5 Capacitance values of the samples.
27

28 (a), sample of (850-850); (b), sample of (850Fe-850); (c), sample of (500Fe-850).
29
30

31 Fig. 6 Nyquist plots for the samples.
32

33 (a), sample of (850-850); (b), sample of (850Fe-850); (c), sample of (500Fe-850).
34
35
36
37
38

39 Fig. s1 Optical microscope image of the bamboo powder.
40
41

42 Fig. s2 Relation between capacitance values and specific surface area of the samples.
43
44
45
46
47
48
49
50
51
52
53
54
55
56
57
58
59
60
61
62
63
64
65

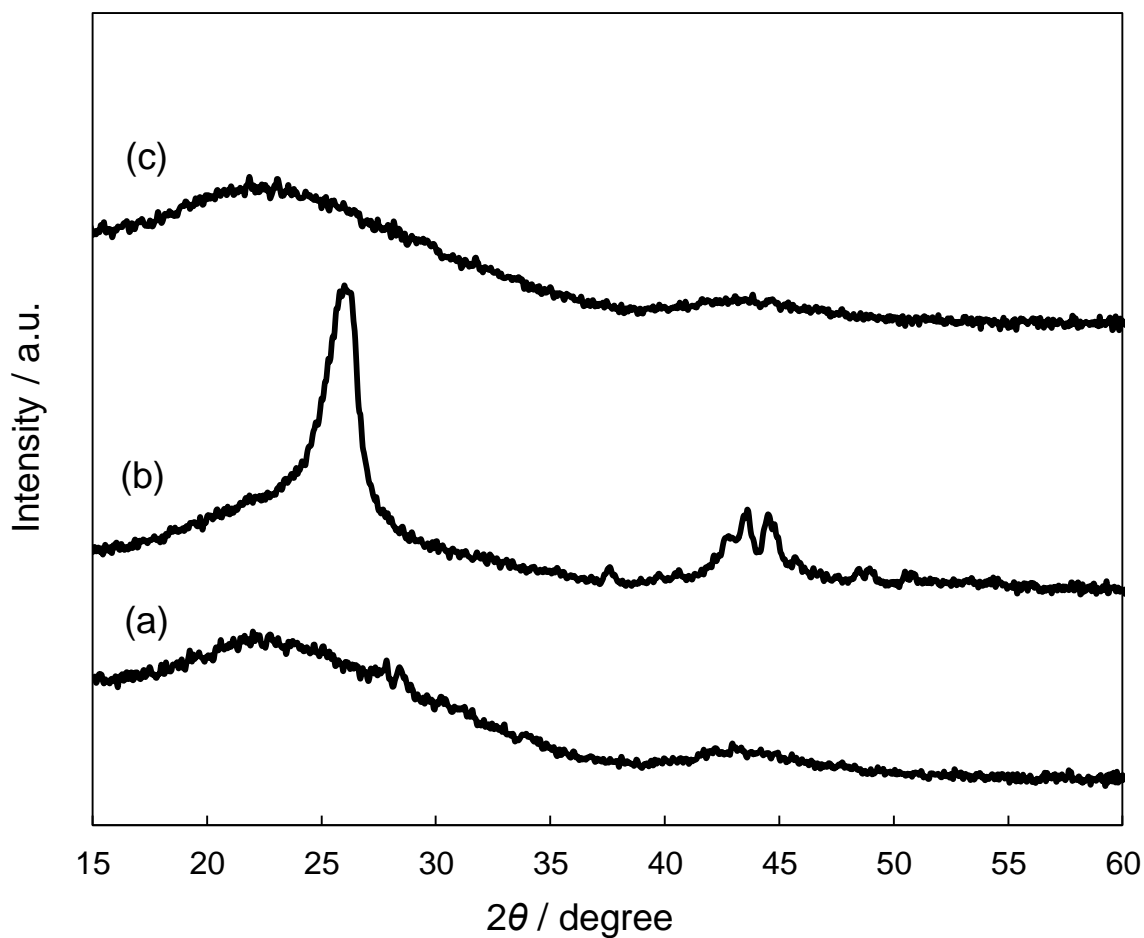


Fig. 1 XRD patterns of the samples.

- (a), sample of (850-850);
- (b), sample of (850Fe-850);
- (c), sample of (500Fe-850).

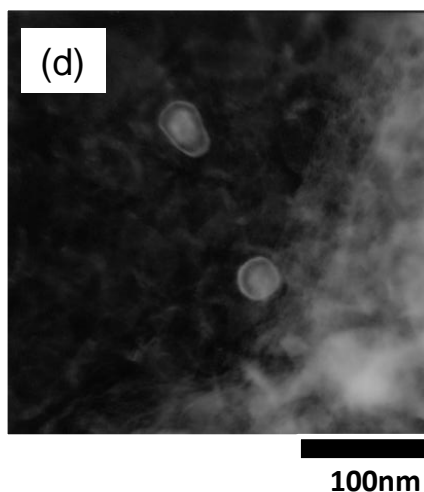
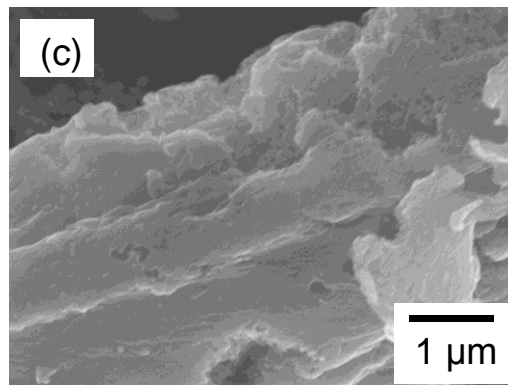
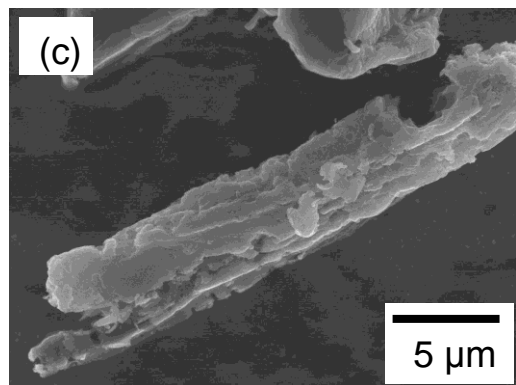
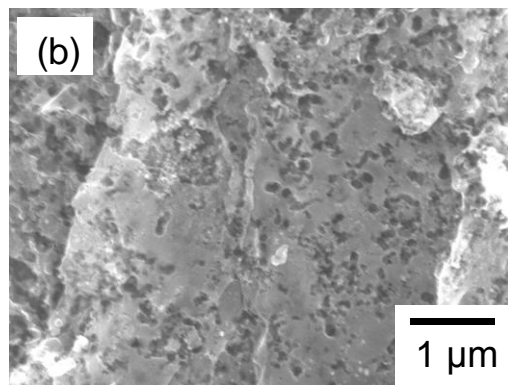
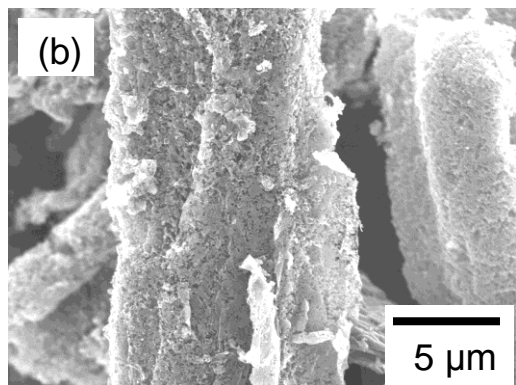
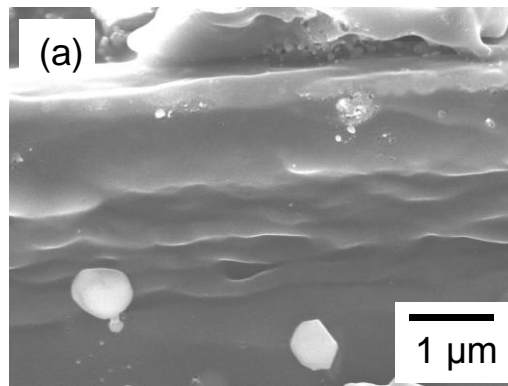
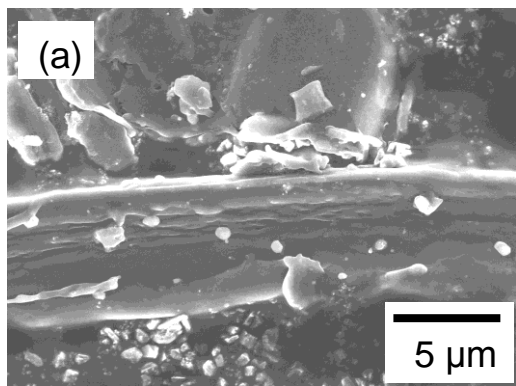


Fig. 2 SEM and TEM images of the samples. (a), sample of (850-850); (b), sample of (850Fe-850); (c), sample of (500Fe-850); (d), TEM image of sample of (850Fe-850).

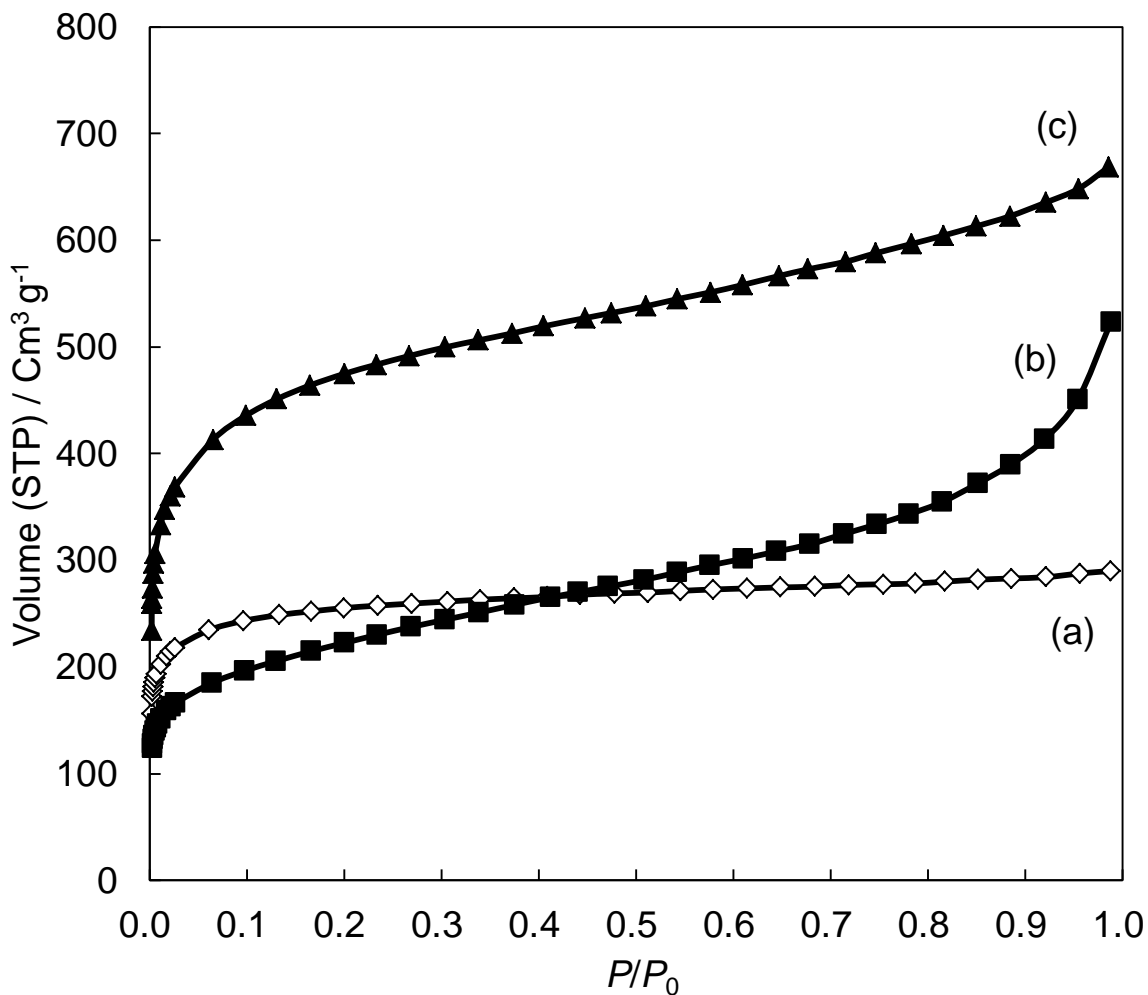


Fig. 3 N₂ adsorption isotherms of the samples.

- (a), sample of (850-850);
- (b), sample of (850Fe-850);
- (c), sample of (500Fe-850).

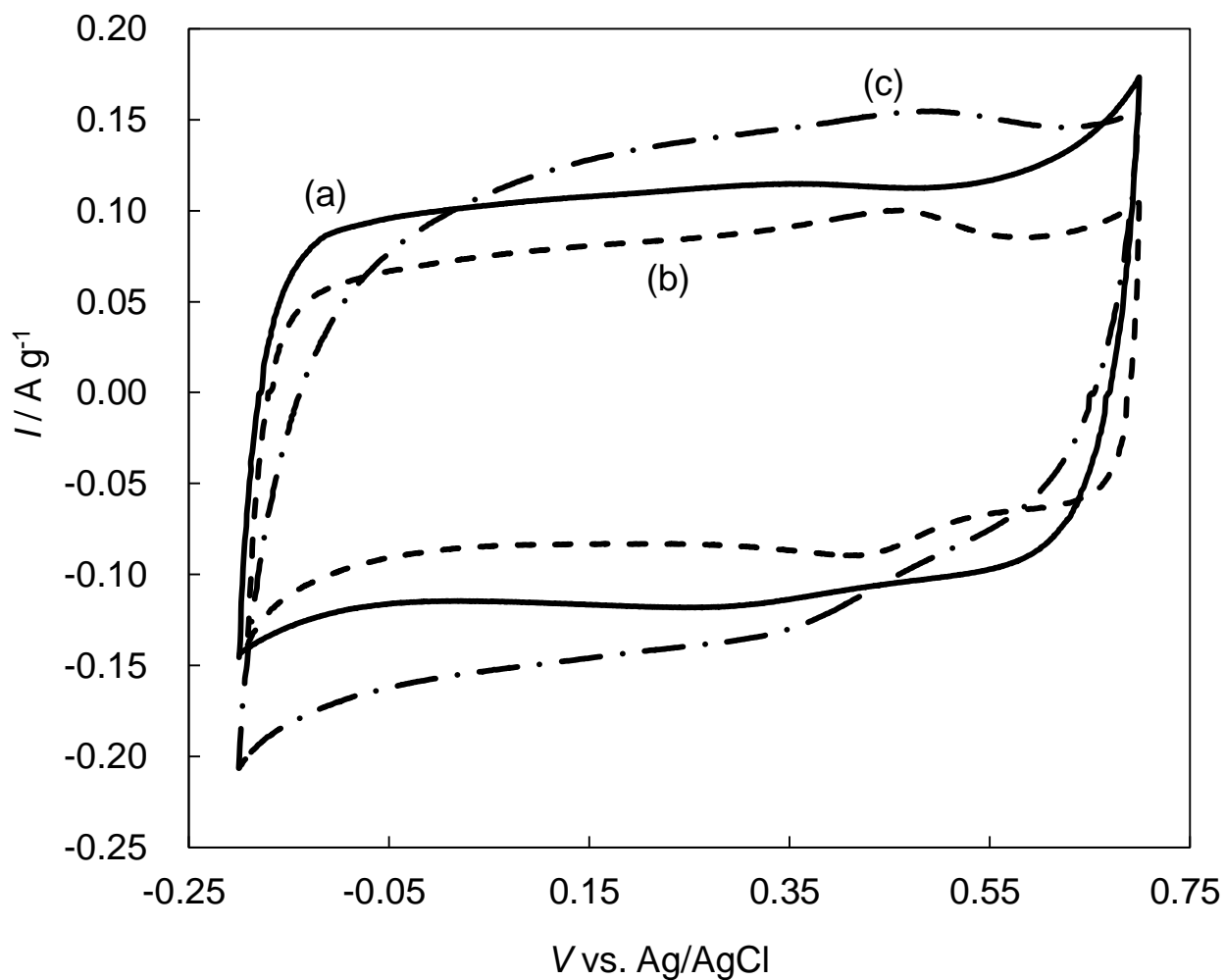


Fig. 4 CV graphs of the samples.

- (a), sample of (850-850);
- (b), sample of (850Fe-850);
- (c), sample of (500Fe-850).

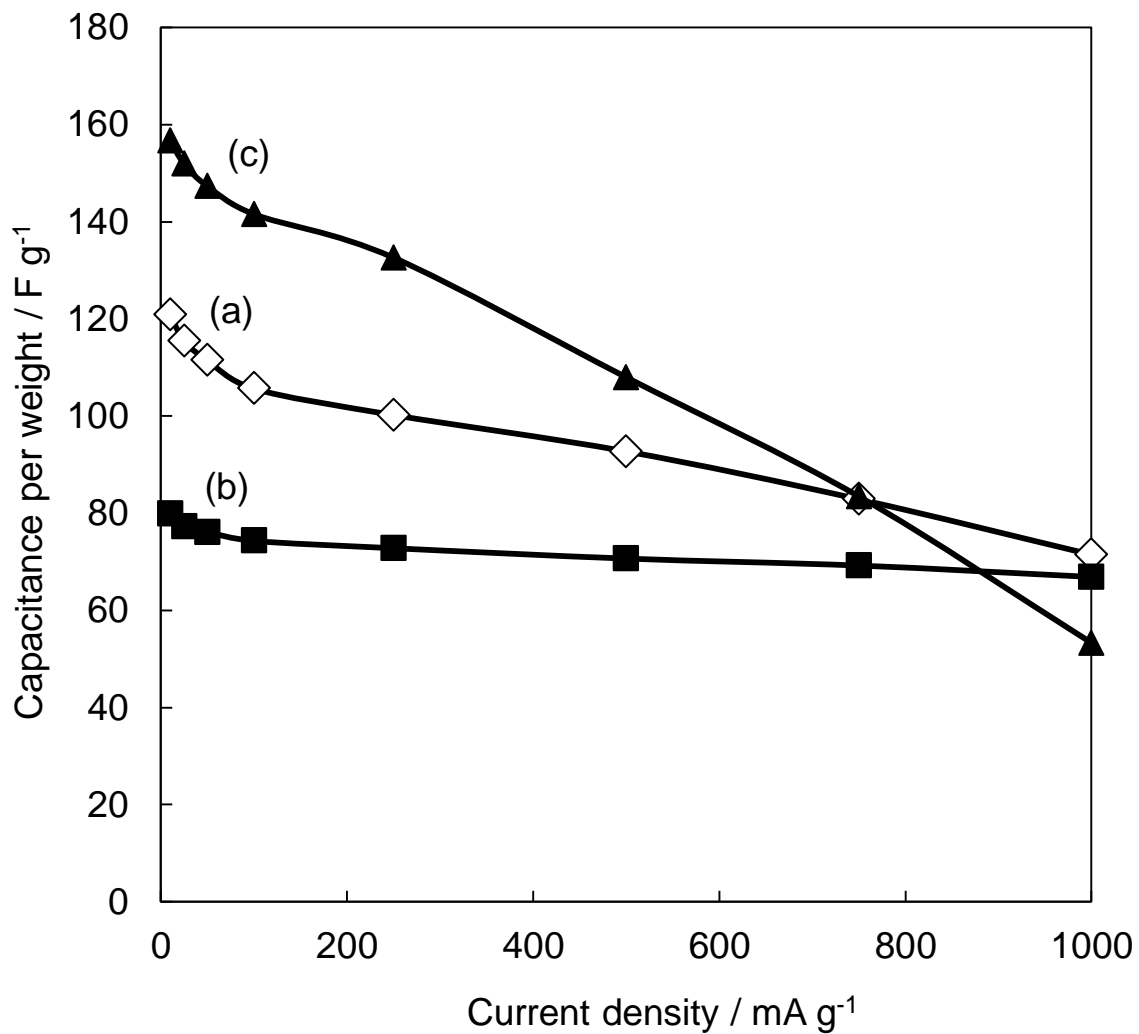


Fig. 5 Capacitance values of the samples.

- (a), sample of (850-850);
- (b), sample of (850Fe-850);
- (c), sample of (500Fe-850).

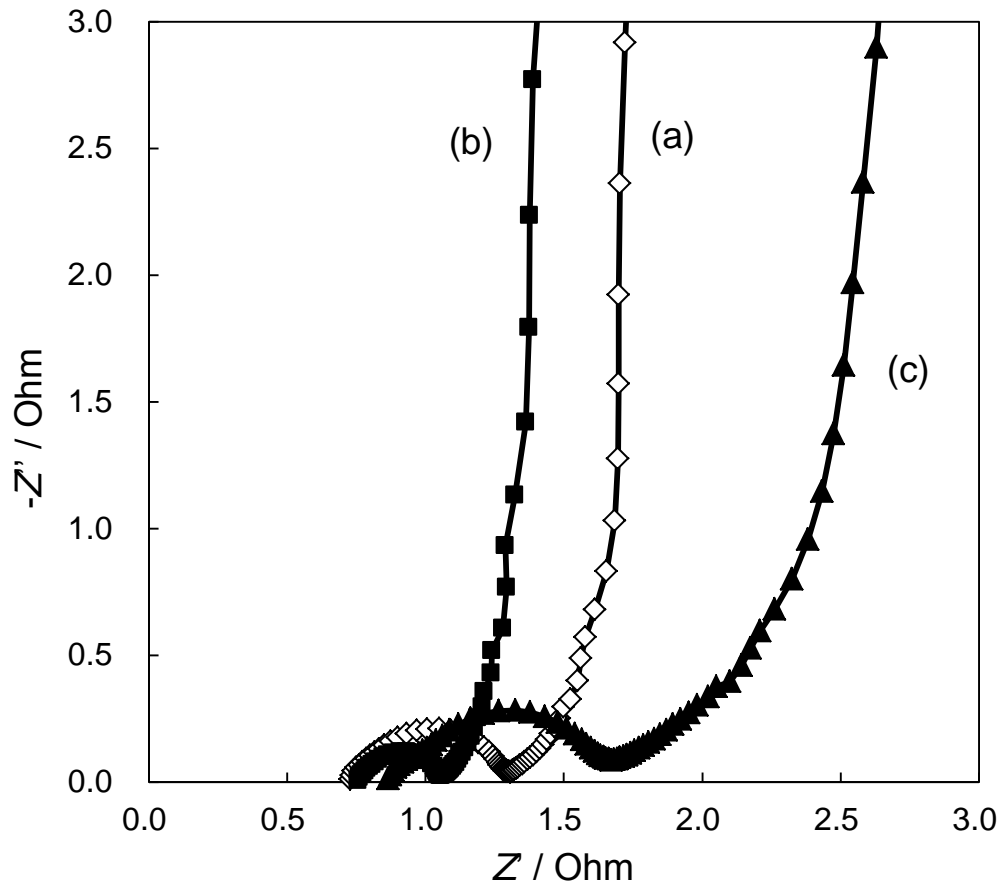


Fig. 6 Nyquist plots of the samples.

- (a), sample of (850-850);
- (b), sample of (850Fe-850);
- (c), sample of (500Fe-850).

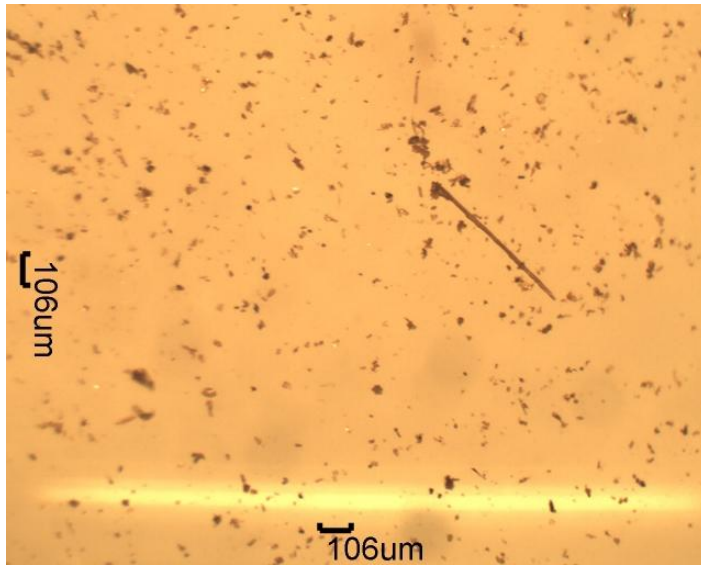


Fig. s1 Optical microscope image of the bamboo powder.

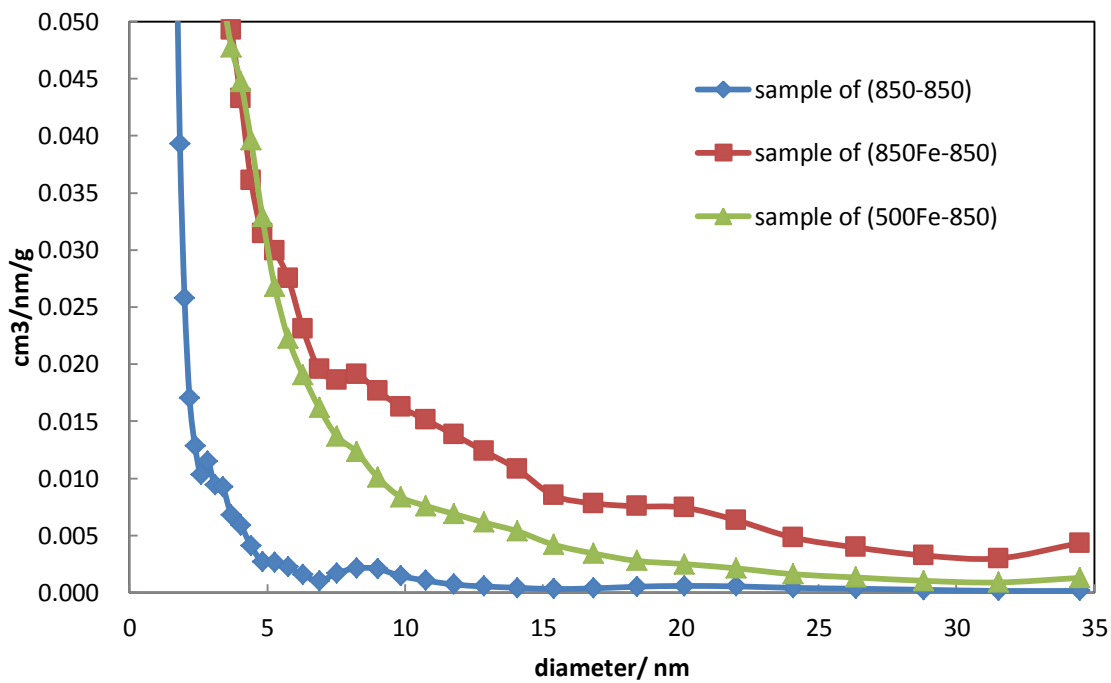
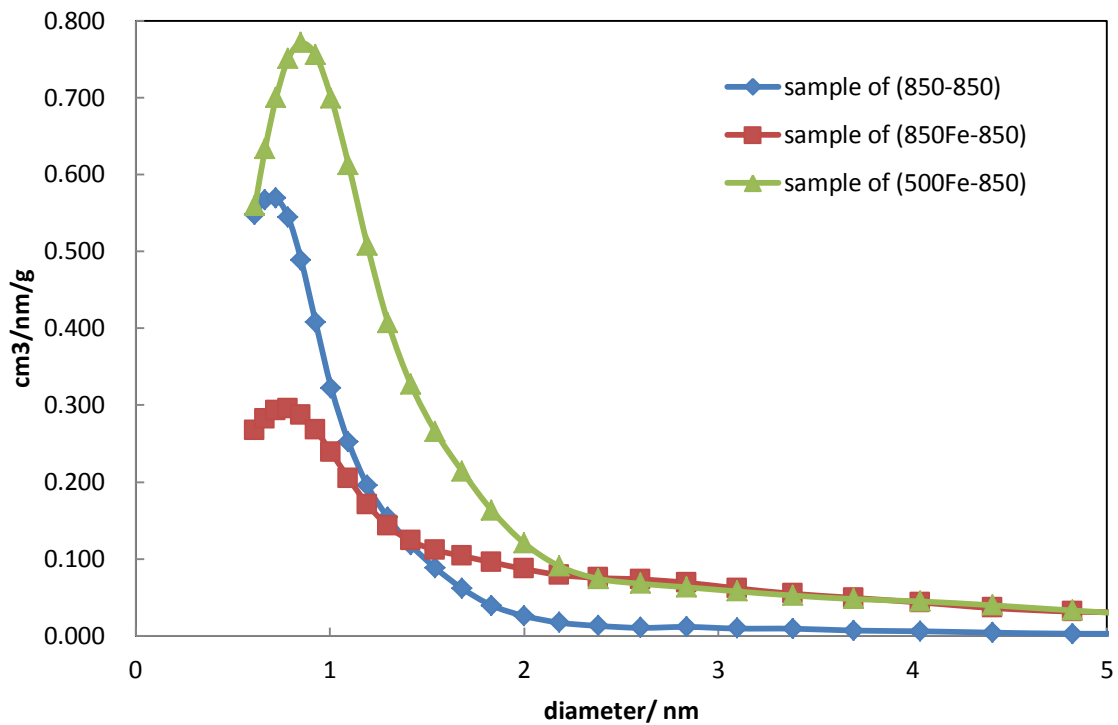


Fig. s2 Pore size distributions of the samples (calculated by DFT method).

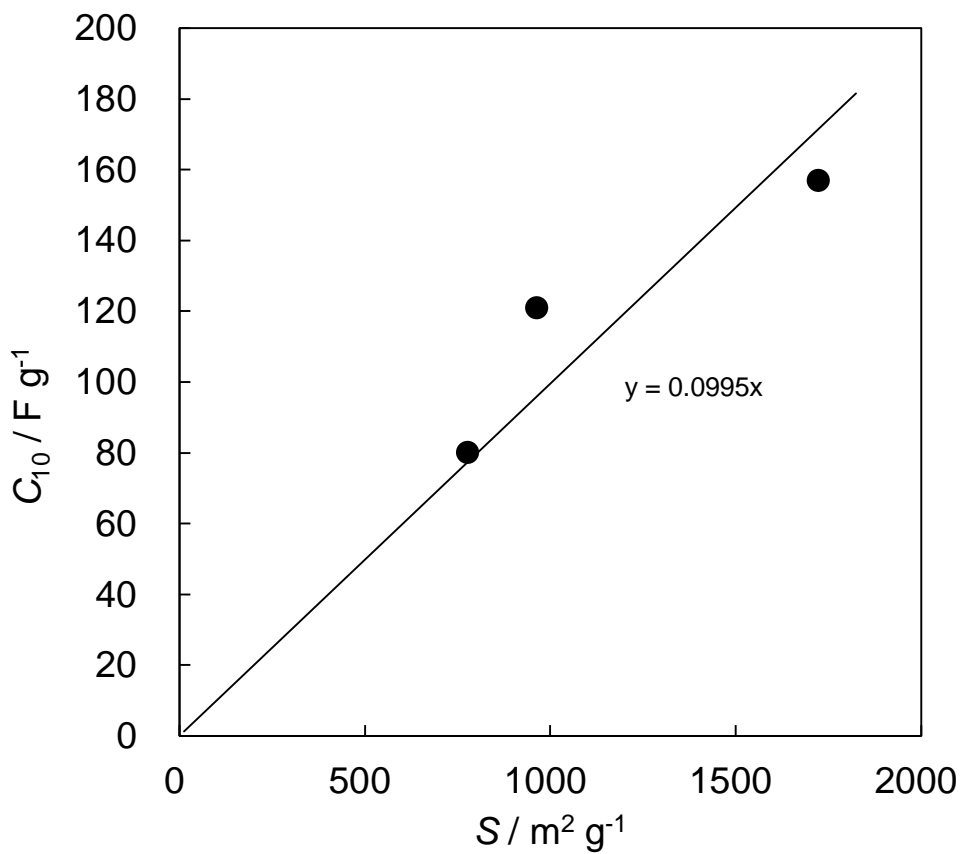


Fig. s3 Relation between capacitance values at 10 mA g⁻¹ and specific surface area of the samples.